Behavior of High Strength Concrete L-Beams Under Combined Bending and Shear

Dr. Omer Q. Aziz * & Ferhad R. Karim**

Received on: 19/2/2006
Accepted on: 26/11/2006

Abstract

This investigation examines experimentally and statistically the behavior and ultimate strength of L-shape reinforced high strength concrete beams under combined bending and shear· The experimental investigation consists of casting and testing of nine beams which were tested under bending and shear. The effect of compressive strength, longitudinal reinforcement on the load carry capacity and the effect of transverse reinforcement on the shear strength is studied· An increase in compressive strength by (65.56%) causes an increase in load carrying capacity and shear strength at cracking load by (21.47% and 162.9%) respectively. An increase in longitudinal reinforcement ratio for bending by (153.8%) caused an increase in load carrying capacity by (46.37%) when the longitudinal reinforcement ratio is kept constant, an increase in transverse reinforcement index by(59.25% %) causes an increase in shear strength at ultimate load by (6.55 %).

By using multiple nonlinear stepwise regression method, based on data in this research and from other literature; equations were proposed for predicting shear strength at cracking and ultimate loads· These proposed equations show good agreement and they are conservative when compared with equations given by Codes of practice.

Keywords: High strength concrete, L-shape beam, bending and shear.

سلوك العتبات ذات مقطع L مصنوعة من كونكريت عالية المقاومة تحت عزوم و قص

الخلاصة

لدراســـــة سلوك ومقاومة العتبات تحت تاثير الانحناء والقص , تم صـــب و فحـــص تسعة عتبات خرسانية مسلحة مصنوعة من الخرسانة عالية المقاومة مع اخذ بنظـــر الاعتبار نسبة تسليح الطولي، ومؤشر التسليح العمودي و نسبة المسافة بـــين تســـليح القص الى العمق الفعال للعتبة. الى زيادة مقاومة الانضغاط بنسبة ٦٥،٥٦% يـــؤدي الى زيادة في القاومة القصوى و جهد القص بمقـــدار ٢١،٤٧ و ١٦٢،٩ % علـــى التوالي. اذا كان التسليح العمودى ثابتا,فـــان زيـــادة نســـبة تســـليح الافقـــى بمقـــدار (١٥٣،٨%) يؤدي الى زيادة في المقاومة القصوى بمقدار (٤٦،٣٧%) .اما اذا كان التسليح الافقي ثابتا، واضيف التسليح العمودي بمقدار(٥٩،٢٥%) فهذه الاضافة تزيد من جهد القص الاقصى بمقدار (٦,٥٥ %).

اعتمادا على البيانات الموجودة لهذا العمل و الابحاث الاخرى, اقترحت بعض المعادلات للتنبأ بجهد القص الاقصى وجهد القص المسببة للشقوق مع عزم الانحناء الاقصى وعزم الانحناء المسبب الشقوق. و هذه المعادلات المقترحةاظهرت نتائج جيدة عند مقارنتهـــا مع معادلات اخرى.

https://doi.org/10.30684/etj.25.2.19
2412-0758/University of Technology-Iraq, Baghdad, Iraq

Introduction:

ACI committee 363 [1] defined high strength concrete (HSC) as a concrete having 28 days cylinder compressive strength exceeding 41 MPa and it excludes concrete made from exotic materials or exotic techniques.

Mphonde and Frantz [2] (1984) have carried out shear tests on high and low strength concrete beams without stirrups, for this purpose they tested nineteen beams to determine their diagonal cracking strength and ultimate shear capacities. Variables in their study were compressive strength and shear span to effective depth ratio, all the beams have rectangular cross section, and they were simply supported under bending and shear. They concluded the followings:

1. At a/d ratio of 3.6, the current ACI equations for shear design (11-3 &11-6) are conservative. However, the ratio measured to predict capacity by using equation (11-6) decreases from 1.64 to 1.20 if $f'c$ increases from 20.685 to 103.425 MPa.
2. Based on the regression analysis, they proposed the following equation:

$$v_u = 0.366 \sqrt[3]{f'c} + 0.49$$

(in MPa) … (1)

Best description of ultimate shear strength is obtained at a/d = 3.6, with standard error of 0.06895 MPa.

3. At a/d of 2.5, ACI-Code equation (11-29) is a reasonable estimate of the lower bound measured shear capacity.

$$v_u = (3.5 - 2.5M/V.d)\left(0.16\sqrt{f'c} + 17.2 r_w \frac{V.d}{M}\right)$$

(in MPa) …(2)

4. At a/d of 1.5, ACI-Code equation (11-29) under-estimates even the lower bound measured shear capacity by 71% for HSC.
5. The effect of concrete strength on the shear capacity becomes more significant as the a/d ratio decreases.
6. Failure becomes more sudden and explosive as $f'c$ increases, especially at lower a/d values.

Elzanaty et al [3] (1986) studied the shear capacity of reinforced HSC beams; in their study they cast fifteen beams without web reinforcement and three beams with web reinforcement. According to the ACI Code 318-83, the total nominal shear strength (V_n) is taken equal to the sum of the contributions of the web reinforcement (V_s) and shear strength provided by concrete (V_c). They concluded the following points: -

1. ACI-Code equation (11-3) is seriously unconservative for beams without stirrups having high $f'c$ and a/d, ranged between (21-83 MPa) and (2-6) respectively with low r_w.
2. The steel ratio below which ACI Code equation (11-6) being unconservative was higher for high strength than for lower strength concrete.
3. ACI Code equation (11-6) underestimates the importance of both r_w & a/d, and overestimates the benefits of increasing $f'c$.
4. For all test beams with stirrups, the concrete contribution to shear strength Vc was higher than that assumed by ACI -Code procedure.

Ahmad ,et al [4] (1986) studied shear capacity of reinforced HSC beams, for this purpose they cast and tested thirty-six reinforced concrete beams using HSC to determine their diagonal

cracking and ultimate shear capacities. The main variables taken into account were the longitudinal reinforcement ratio, and shear span to depth ratio while the secondary variable was compressive strength ($f'c$). An equation was proposed to predict the ultimate shear stress:

$$v_u = h\left[50\left(f'_c * r_w * d/a\right)\right]^{0.333}$$

for $3 \le a/d \le 6$ … (3)

where:

h : Depth factor, $h = 1 - 0.0414\left[(d - 5.35)^{0.85} / \left(a/d\right)^{0.63}\right]$ The ACI-Code equation (11-3) is conservative for beams with low shear span to depth ratios, that is; a/d<2.5. Equation (3) is unconservative for HSC beams with a low percentage of (r_w).

Sarsam et al [5] (1992) studied shear design of high and normal strength concrete beams; for this purpose they examined fourteen beams with stirrups failing in shear. The variables taken were the compressive strength, shear span to effective depth ratio $a/d \ge 2$, ρ_w, and $\rho_v \cdot f_{yv}$, all the beams have rectangular cross-section. They proposed the following equation to determine shear resistance:

$$v_{rprop} = 0.85\left[1.8\left(f'_c \cdot r_w \cdot v_u \cdot d/M_u\right)^{0.38} b_w \cdot d + \frac{A_v \cdot f_y \cdot d}{s}\right]$$

… (4)

They concluded the following points:-

1. The proposed equation (4) and ACI-Code equation (11-6) are conservatives for HSC and NSC beams.
2. The proposed equation (٤) and ACI-Code equation (11-6) does not give lower the safety factor of the ACI-Code or the proposed equation for fc' up to 82.9 Map.

Buni Z.K. [6] (1994) studied shear strength of HSC beams; they studied the effect of the following variables on shear strength provided by concrete:

1. Shear span to depth ratio which ranged between (2.5 & 6).
2. Aggregate interlock &dowel action.
3. Longitudinal reinforcement ratio which have ranged between (3.1 &6.5)%.

They concluded the following points: -

1. Shear strength of beams decreased when a/d increased.
2. The small amount of stirrups led to a significant drop in the brittleness of shear failure as well as (10-20 %) increase in shear capacity.
3. The surface of inclined crack was smooth for HSC. These smooth cracks reduced the value of aggregate interlock and shear transfer mechanism from 33% to 50 % for NSC beams, while they reduced from 8% to 13 % for the HSC beams. They proposed an equation to determine the shear strength of high strength reinforced concrete beams with web reinforcement as follows:

$$V_u = jV_c + j\left(r_v * f_{yv} * (a/d)/\int (a/d)\right) b_w * d$$

…(5)

$$jV_c = \left[2.5\left(f_{c'} * r_w * d/a\right)^{0.386}\left(4 - 1.2a/d\right)\right] b_w * d$$

…(6)

Where: $\left(4 - 1.2\,a/d\right) \ge 1.0$

Research significance:

This research applied to study:

1. The effect of compressive strength on load carrying capacity of reinforced high strength concrete L-shape beams.

2. The effect of longitudinal reinforcement ratio on load carrying capacity of reinforced high strength concrete L-shape beams.

3. The effect of transverse reinforcement index on shear strength of reinforced high strength concrete L-shape beams.

Experimental Program:

Detail of the specimens:

All the tested specimens have the dimensions of about (b_w=220mm, b_f=320mm, h=300mm, hf=110mm and L=2200mm), these dimensions are identifiable with ACI Code specification as shown in Fig. (1). Different methods for distribution of the longitudinal steel bars can be observed in two layers in shear span only as shown in Fig. (2).The tested specimens were divided into two groups [A and B] as listed in Table(1) .

The variable of beams in group [A] is the longitudinal reinforcement for bending ranging between minimum longitudinal reinforcement for bending to 0.991% with compressive strength ranging between (30-60) MPa. The beams in this group were designed to fail in bending. The variables of beams in group [B] are the transverse reinforcement index for shear ($\rho_v.f_{vy}$) which ranged from 0 to 1.739 MPa and the beams were designed to fail in shear.

Mixing detail:

Mix proportion:

Mix proportion for production of high strength concrete requires more quality control than normal strength concrete (NSC), usually chemical admixtures are essential for using low w/c ratio. Many trial mixes are often required to generate the data necessary to identify the optimum mixture proportions. In this study the initial proportions were based on those attained by Buni [6] & Aziz [7]. The following steps were followed: -

A .The fine and coarse aggregate were sieved, washed to remove the dust and then air dried.

B. Slump tests were made on different mixes having different amounts of cement content in the first series which ranged between (492.5 to 611.5 kg/m^3) without admixture and the second series having different amount of cement ranging between (541.5 to 583 kg/m^3) with admixture. The suitable dosage of admixture (0.35%) of the weight of cement was selected, different ratio of sand to the total aggregate (0.3 to 0.4) were used in these mixes in order to find the W/C ratio that gives different slump between (5- 100 mm).

C. Trial mixes were made, the aggregate to cement ratio ranged between (2.6 & 3.175) and the mixes selected to give fc' from 30 to 60 MPa with slump ranged between 5-100mm.

The following equation can be solved for the total aggregate weight, knowing the weight of cement, water and the bulk specific gravity of the materials:

$$\left(\frac{W_w}{g_w}\right)+\left(\frac{W_c}{g_c}\right)+\left(\frac{W_s}{g_s}\right)+\left(\frac{W_g}{g_g}\right)+\left(\frac{W_{Ad}}{g_{Ad}}\right)=1 \quad \ldots (7)$$

where: W_w, W_c, W_s, W_g & W_{Ad} are weight of water, cement, sand, gravel and admixture respectively. γ_w,γ_c, γ_s , γ_g and g_{Ad} : are the bulk specific gravity of water, cement, sand , gravel and admixture respectively. Air voids in the mix is assumed small and neglected.

D. For each concrete mix six cylinders (150X300mm) were cast; three of them tested at age of 7 days and the others at age of 28 days. The cylinders were cured by immersing in tap water, which is saturated by lime, and then dried in the laboratory temperature and humidity by one day before testing.

E. Some of mixing process for the trial mixes were done by hand (manually).

F. Then the mix proportions for beams selected to obtain different compressive strength were as shown in Table (2).

Mixing method:

The mixing procedure is important for obtain uniform mix. A (0.08 m^3) tilting mixer was used and the following sequence was adopted during mixing. The interior surface of the mixer was cleaned and moistened before placing the materials; initially the coarse aggregate and fine aggregate were put in the mixer, followed by 25% of the mixing water with admixture to wet them. Then the cement was added, followed by 75% of the remaining water with admixture .The mixing operation continued until uniform mix obtained.

Fabrication of reinforced concrete beams:

Steel plate forms were used in the fabrication of the molds for the specimens. The form was made of 2 mm steel plate, as shown in Fig. (3).After removing the specimen from the molds, they was cleaned, re-assembled and oiled for the next pour. The reinforcement gages were prefabricated and fixed in the form and the movement was avoided during casting of the beams.

Casting and curing:

Casting was started by placing the mixture inside the molds of beams using a trowel, the mixture was placed in three layers and each layer was vibrated for about 20 seconds using internal vibrator in four locations spaced about 50 cm from one to another. The vibration was applied for all layers, the top layer was vibrated until the number of bubbles appeared on the surface was reduced and finished with a steel trowel. After five hours the molds were covered with damp canvas cloth and left in the laboratory for about twelve hours. Then the specimens were taken out from the molds and covered with damp canvas for twenty eight days after that left in air temperature and humidity until date of testing.

Test measurements :

Load measurements:

The reinforced concrete beams were tested using [Avery] testing machine of eighty-ton capacity. The beams were restrained at both ends, loaded by two point loads and the distance between two applied loads was fixed (400mm) in order to keep the ratio of shear span to depth constant.

Deflection measurements:

Vertical deflections were measured at the mid-span of the

beams and under the point loads using a dialgauge of (30) mm with a minimum reading of (0.01) mm.

Rotation measurement:

The angle of twist was measured from deflection measurement at a distance 65 mm from center of the rectangular section at location of the point loads.

Supports:

The supports at both ends of beams were restrained for bending and fixed for shear.

Testing procedure:

The beams were prepared one day before testing, and were painted by white color prior to testing in order to view crack propagation. The beams were tested with a span between two point loads of [40 cm] in order to transfer the applied point loads. Initially zero load readings for the electrical strain gauges as well as the dial gauges were taken and recorded. The load magnitude for each load stage was chosen according to the expected strength of the beam. At each load stage the dial gauge readings were taken.

Magnifying glass was used to locate the cracks at each load stage. The inclined cracking load and spiral cracking load (if present) were reported. The testing continued until the beam showed a drop in loading with increasing deformation.

Discussion of the test results:

Effect of concrete compressive strength (f'c):

For beams in group [A], cracking shear strength is increased by (162.9 %) with an increase in compressive strength by about (65.56 %) as shown in the Fig.(4). Load carrying capacity has been affected by compressive strength of concrete as shown in Fig. (5), (longitudinal reinforcement ratio was constant), where an increase in compressive strength by (65.56%) caused an increase of load carrying capacity by about (21.47%).

Effect of longitudinal reinforcement ρ_w:

The effect of longitudinal reinforcement on the load carrying capacity is shown in Fig.(6) ,an increase in longitudinal reinforcement ratio by about (153.8%) caused an increase in load carrying capacity by about (46.37%) after subtracting the effect of compressive strength of concrete.

Effect of transverse reinforcement index ($\rho_v.f_{vy}$) :

The effect of transverse reinforcement index for shear on shear strength after subtracting effect of compressive strength and dowel action[5] is shown in Fig.(7).Increasing in ($\rho_v.f_{vy}$) by about (59.25%) caused an increase in shear strength by about (6.55%) as given in Table(3).

Load and mid-span deflection relationship: -

Deflections of the tested beams in group A and B were measured at mid span and the loads versus deflection of these groups are plotted in Figures. (8, 9 and 10).

For group [A], the relations indicate that the ultimate deflection increases due to an increase in longitudinal reinforcement. In Fig. (8) it is shown that the values of deflection at ultimate load are larger for the beam with large amount of longitudinal reinforcement, an

increase in longitudinal reinforcement by about [114% and 153%] causes an increase in deflection at ultimate load by about [48.9% and 90.78%] respectively.

Crack patterns and modes of failure:

Cracks in the concrete beams were formed generally in the regions where the induced tensile stress in specimens exceeds the tensile strength of concrete. One type of crack was observed in the tested beams in group **[A]**. As shown in Fig. (11), these cracks were formed from flexural tensile stresses in the region between two point loads. For beams in group [**B**], two types of cracks were observed as shown in Fig.(12); the first type of crack was the flexural crack between two point loads, and the second type of crack was the shear crack which is formed as a result of the inclined tensile stresses acting on the web of the beam in the region of shear span (combined bending and shear). Beam **[A3]** shown in Fig. (11) failed in flexure according to the following sequences:-

1. Shear-flexure cracks are formed at the shear span.
2. Cracks propagation continued between two-point loads and approached the compression zone.
3. With further loads the cracks extended in two directions, the first one towards the compression zone and the second one chased an inclined path towards the supports.
4. After that the cracks extended in the compression zone in the pure moment region and at support towards the point loads causing failure.

For beams in group [**B**] the same as group [**A**] but with greater propagation of cracks in shear span was observed and failed when the second main crack extended in inclined path towards the supports and under further load failure occured .

Prediction equations for reinforced concrete beams:

The parameters d/bw, da/db, s/d, s/Ab, a/L, a/d, r_w, r_v fvy fc', and concrete cover at bottom face were accounted for predicting the statistical equations. New empirical constants were calculated using the test results from other literature [2, 3, 4, 5, 6, 8,9, 10, 11 and 12] in addition to data from this work. These equations were tested by evaluating (experimental to predicted value ratio) for ultimate and cracking shear strength, cracking bending moment then standard deviation, standard error, coefficient of variation, and coefficient of determination were evaluated for these equations.

Reinforced high strength concrete beams under bending and shear with stirrups:

Cracking shear stress:

In addition to the present work (3 beams), results of (9) reinforced HSC, intermediate length beams from other literatures [2, 5,& 9] failed under shear and bending loads, were taken to predict the proposed equation. Multiple nonlinear stepwise regression method was adopted to relate the cracking shear stress in terms of the effective parameters.

The general equation for predicting cracking shear stress is:

$$u_{cr} = \frac{1.6433}{\left(\frac{L}{d}.\frac{s}{d}.r_w.\frac{d_a}{d_b}.\frac{d}{b_w}\cdot f'c\right)^{0.02254}} \quad \text{(MPa)} \quad \ldots (8)$$

Ultimate shear stress:

Results of [11] reinforced HSC beams; intermediate length beams from other literatures [2, 5 and 9] in addition to the three beams in this work were used to predict equations for the ultimate shear stress. Nonlinear multiple stepwise regression was used to predict ultimate shear stress.The general predicted equation is:

$$u_u = 3.995\left(f_{c'}.r_v.f_{vy}\cdot\frac{d_a}{d_b}\cdot b_w\right)^{0.00159} \quad \text{(MPa)} \quad \ldots (9)$$

Reinforced high strength concrete beams under bending and shear without stirrups:

Cracking shear strength:

In addition to one beam in this work, 46 beams are taken from the literature [3, 4, 5,6, 8 & 11].

Multiple nonlinear stepwise regressions is used to represent cracking shear strength. The best description for cracking shear strength of beam without shear reinforcement is:

$$v_{cr} = 60.845\left(\frac{d}{f_{c'}}\right)^{0.00457} \quad \text{(MPa)} \quad \ldots(10)$$

Ultimate shear stress:

The multiple nonlinear stepwise regression analysis is used to describe equation for predicting ultimate shear stress of one beam in this work with [57] beams from other literatures [3, 4, 5, 6, 8 and 11], and the best equation is:

$$u_u = 1.2244\ (r_w)^{0.508358} \quad \text{(MPa)} \quad \ldots(11)$$

Evaluation of the proposed equations:

Reinforced HSC beams under bending and shear with shear reinforcement:

- **Cracking shear stress:**

The cracking shear stress is calculated by the proposed equation. The ratios of v_{cr} by experiment to that predict by the proposed equation are calculated as listed in Table (4).

- **Ultimate shear stress:**

The ultimate shear stress is calculated by the proposed equation. The predicted results were compared with some practical code equations as listed in Table (5).

Reinforced HSC beams under shear and bending without shear reinforcement:

- **Cracking shear strength:**

The cracking shear strength which has been calculated by the proposed equation was compared with design equations in codes of practice and listed in Table (6).

- **Ultimate shear stress:**

The ultimate shear stress predicted by the proposed equation is

compared with codes of practice and some other equations proposed by other researchers and listed in Table (7).

Conclusions:

From the experimental and statistical study the following conclusions are reached:

1. An increase in compressive strength by (65.56%) causes an increase in load carrying capacity by (21.47 %).

2. An increase in longitudinal reinforcement ratio for bending by 153.8% causes an increase in load carrying capacity by 46.37 %.

3. An increase in transverse reinforcement index by (59.25%) causes an increase in shear strength by (6.55 %) after subtracting the affect of compressive strength and dowel action.

4. The proposed statistical equations show good agreement when compared with the proposed equations given by codes of practice such as (ACI, Canadian, and BS) codes and those proposed by other researchers, so the proposed equations can be used as design equations.

References:

1. ACI Committee 363 "State-of-the-Art Report on High-Strength Concrete," (ACI 363R-92), American Concrete Institute,Detroit, 1992, 59 pp.
2. Mphonde, A.G. and Frantz, G.C. "Shear Tests of High and Low Strength Concrete Beams without Stirrups," ACI Journal, V.81, July-August, 1984,pp. 350-357.
3. Elzanaty, A.H., Nilson A.H. and Slate F.O. "Shear Capacity of Reinforced Concrete Beams using HSC," ACI Journal, V.83, March-April, 1986, pp.290-296.
4. Ahmad, S.H., Khaloo, A.R. and Poveda, A. "Shear Capacity of Reinforced High-Strength Concrete Beams," ACI Journal, V.83, March-April, 1986, pp.297-305.
5. Sarsam, K.F. and Al-Musawi, M.J. "Shear Design of High and Normal Strength Concrete Beams with Web reinforcement,"ACI Journal, V.89, Nov.-Dec., 1992, pp.658-664.
6. Buni, Z.K. "Effect of Shear Span to Depth ratio on Shear Strength for HSC Beams, " M.Sc, Thesis, Univ. of Technology, Dec., 1994.
7. Aziz O.Q. "Effect of Revibration time and high temperature on the High Strength Fibrous Concrete Properties,"JDU (sei), V.2, No.5, April, 1999, pp.693-701.
8. Sarsam, K.F. and Abdullah, A.M. "Shear Strength of High Strength Concrete Beams," Al-Mahandis Magazine, No.2, 1989, pp.15-25.
9. Johnson, M.K. and Ramirez, J.A. "Minimum Shear reinforcement in Beams with Higher Strength Concrete," ACI Structural Journal, V.86, July-August, 1989, pp.376-382.
10. Ahmad, S.H. and Lue, D.M. "Flexure-Shear interaction of Reinforced High Strength Concrete Beams," ACI Structural Journal, V.84, July-August, 1987, pp.330-341.
11. Roller, J.J. and Russell, H.G. "Shear Strength of High Strength Concrete Beams with Web Reinforcement," ACI Structural Journal, Vol.87, March-April, 1990, pp.191-198.
12. Barton, T.G. and Kirk, D.W. "T-beams subject to Combined Loading," Journal of the

Structural Division, V.99, No.ST4, April, 1973, pp.687-700.

13- Ferhad R. Karem " Strength and Behaviour of High strength L-beam Under Combined Bending, Shear and Torsion Loading" M.Sc. Thesis, University of Sulaimani, 2004.

Table (1) Details of the specimens

Beam No.	b_f-mm	h_f-mm	b_w-mm	d-mm	f'c-MPa	$\rho_{w-\%}$ at +ve M.S.	$\rho_{w-\%}$ at –ve M.S.	$\rho_{v.}f_{vy}$ MPa	design load $P_{theo.}$-kN
A-I	327	113	223	238	43.32	0.39	0.57	1.092	145
A-I-1	325	109	223	248	36.53	0.39	0.57	1.092	144.1
A-I-2	326	110	222	249	60.48	0.39	0.57	1.092	146.5
A-II	325	115	223	240	51.32	0.84	0.96	1.092	165.7
A-III	327	114	223	239	61.21	0.99	1.25	1.092	204.2
B-I	324	114	223	247	69.19	1.45	2.20	0	148.9
B-II	326	115	222	250	64.21	1.45	2.20	1.097	226.2
B-III	326	115	224	250	57.66	1.45	2.20	1.447	298.9
B-IV	328	114	223	249	78.27	1.45	2.20	1.747	300.8

Table (2) Mix proportions of beams

Beam No.	Mix proportions
	Ad: W: C: S: G
A-I-1	0: 0.50: 1: 0.78: 1.82
A-I-2	0: 0.33: 1: 1.194: 1.854
Others	0.0035: 0.32: 1: 1.175: 2

Table (3) Results of the tested beams *

Beam No.	Type of failure	P_E/P_{th}	P_E	Cracking load	Ultimate load
				kN	kN
A-I	**I**	**1.206**	**175**	**51.90**	**86.9**
A-I-1	**I**	**1.131**	**163**	**30.69**	**82.2**
A-I-2	**I**	**1.351**	**198**	**80.70**	**99.7**
A-II	**I**	**1.545**	**256**	**66.97**	**129.9**
A-III	**I**	**1.449**	**296**	**76.93**	**149.9**
B-I	**II**	**1.462**	**214**	**81.92**	**108.9**
B-II	**II**	**1.228**	**274**	**81.89**	**138.9**
B-III	**II**	**0.902**	**266**	**71.93**	**134.9**
B-IV	**II**	**0.996**	**296**	**84.39**	**149.9**

*: These results include weight of beam and loading structure.

I: bending failure II: shear failure

P_E: Experimental ultimate load –kN, $P_{th.}$: Theoretical ultimate load-kN

Table (4) Comparing cracking shear stress for HSC beams

Pro.equation	R^2	SD	SE	COV-%	AVG
ACI-code	0.990350	0.113703	0.424352	0.1794	1.11687
BS-code	0.998764	0.046856	0.173748	0.0739	1.01913
Canadian code	0.962777	0.184815	0.687884	0.2908	1.55121
Proposed eq.	0.9942	0.0929	0.3470	0.133	1.019

Table (5) Comparing ultimate shear stress for HSC beams

Proposed equation	R^2	SD	SE	COV-%	AVG
ACI-code	0.4933	0.5995	2.3669	0.8261	1.59239
BS-code	0.7538	0.5623	2.2200	0.7749	1.540187
Canadian code	0.1037	0.7250	2.8620	0.9990	2.055511
Proposed equation	0.97223	0.2559	0.9199	1.5867	1.022
Zustti-eq.	0.7488	0.6198	2.4244	0.8540	1.55752
Sarsam eq.	0.9201	0.4611	1.8036	0.6353	1.163953

Table (6) Comparing cracking shear strength for HSC beams

Pro. equation	R^2	SD	SE	COV-%	AVG
ACI-code	0.8599	3.129	21.209	1.329	1.286
BS-code	0.9002	2.510	17.002	1.066	1.070
Canadian code	0.6909	5.158	34.962	2.191	1.786
Proposed eq.	0.7985	5.014	33.993	2.130	1.085

Table (7) Comparing ultimate shear stress for HSC beams

Proposed equation	R^2	SD	SE	COV-%	AVG
ACI-code	0.982526	0.1531	1.1557	0.0715	1.5315
BS-code	0.990628	0.1186	0.8959	0.0549	1.3462
Canadian code	0.961412	0.1904	1.4373	0.0881	2.1271
Proposed eq.	0.996517	0.0842	0.6356	2.7323	1.0365
Zsutti-eq.	0.995599	0.0900	0.6798	0.0417	1.1359
Bazant eq.	0.996817	0.0797	0.6013	0.0369	1.1160

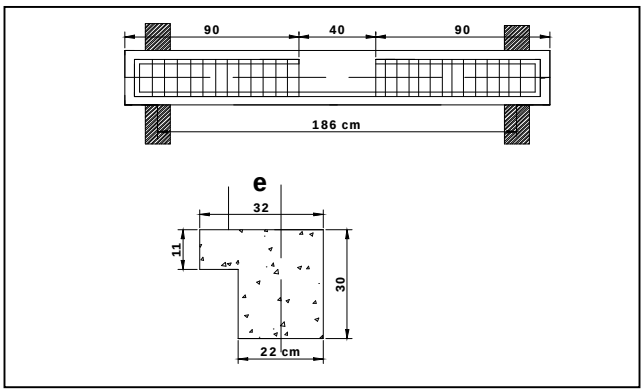

Figure (1) Layout and cross section dimensions of beams

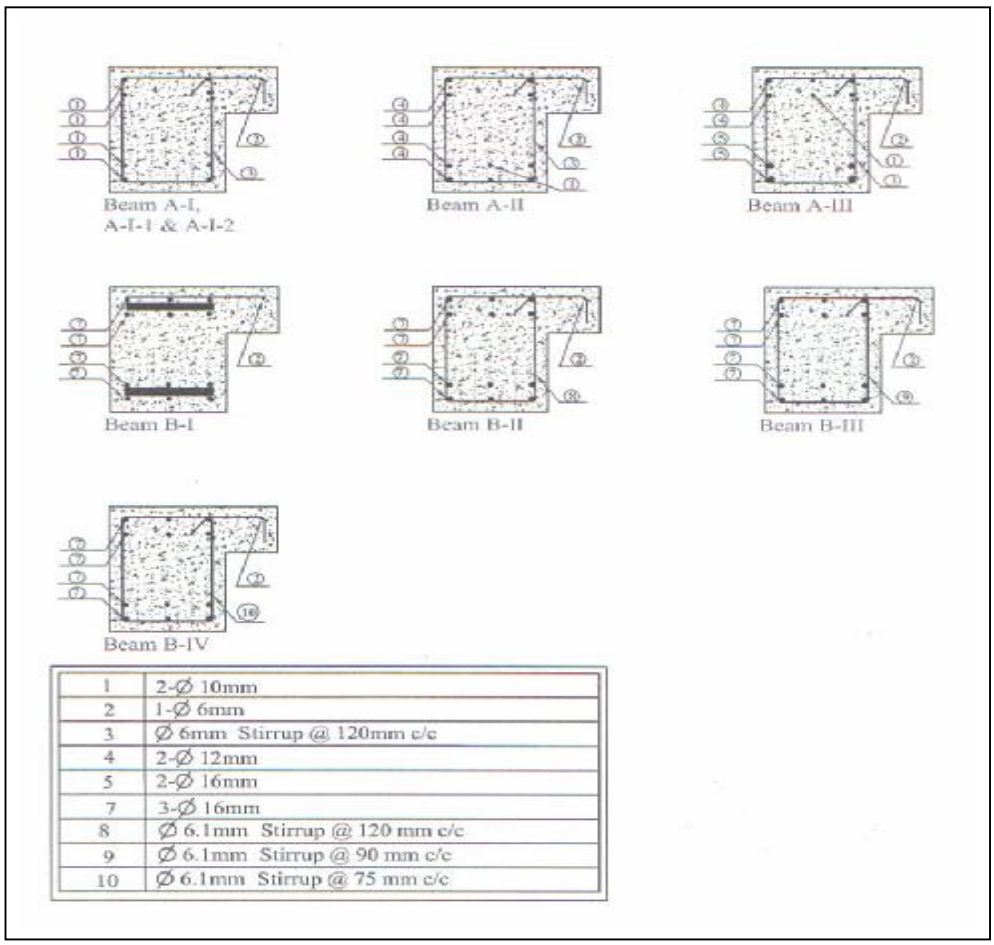

Figure (2) Details of reinforcement for the testing specimens

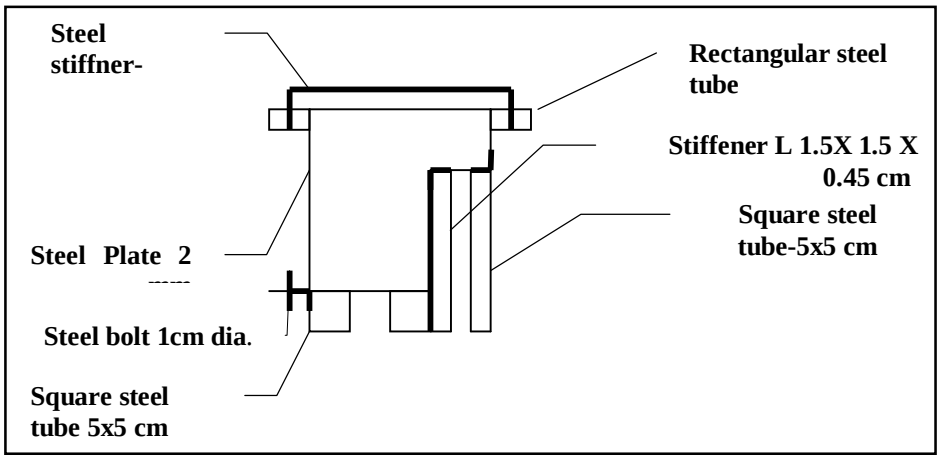

Figure (3) Form work cross section of L-shape specimen

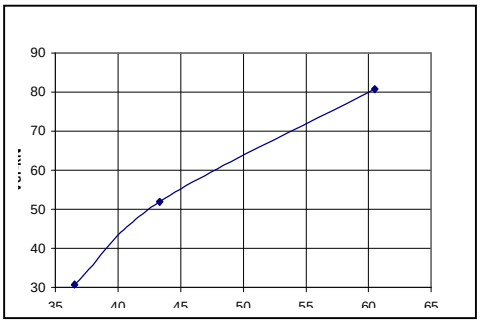

Figure (4) Cracking shear strength versus compressive strength of beams in group A (A-I,A-I-1 and A-I-2)

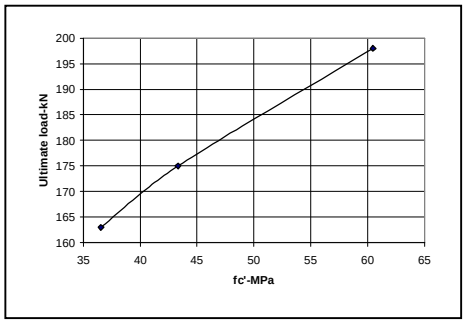

Figure (5) Load carrying capacity versus compressive strength of beams in group A (A-I, A-I-1 and A-I-2)

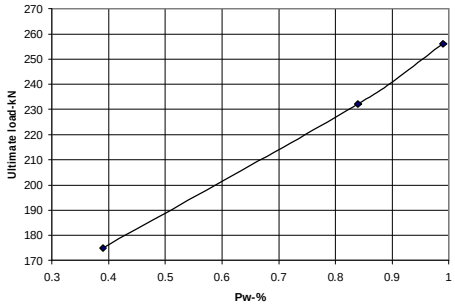

Figure (6) Relation between load carrying capacity and ρ_w-% for group A (A-I, A-II and A-III)

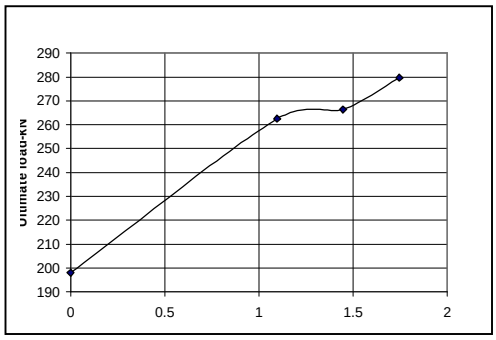

Figure (7) Shear strength provided by stirrups versus ρv.fvy for beams in group B

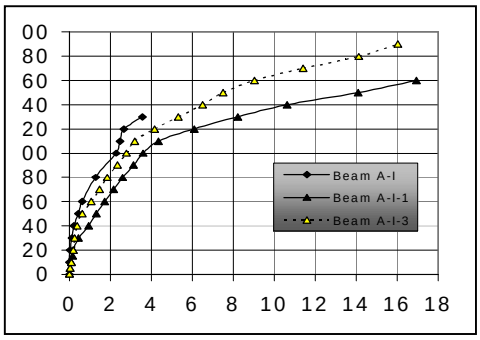

Figure (8) Load and mid span deflection relation for beams (A-I, A-I-1 & A-I-2)

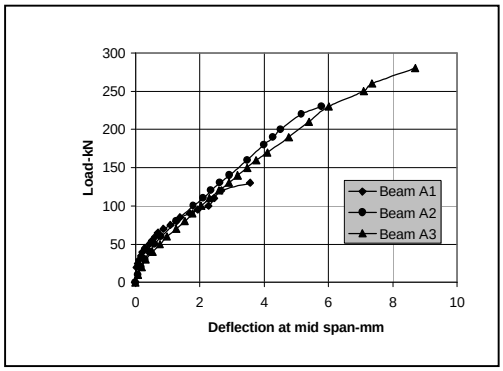

Figure (9) Load and mid-span deflection relationfor beams in group A

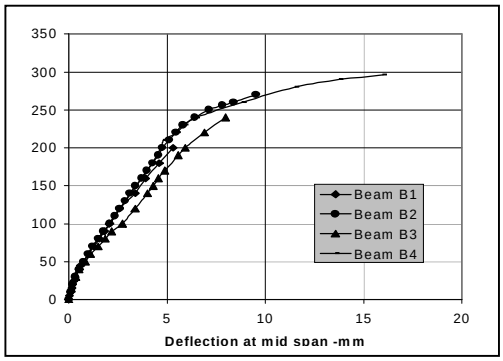

Figure (10) Load and mid-span deflection relation for beams in group B

Side view for beam A-1

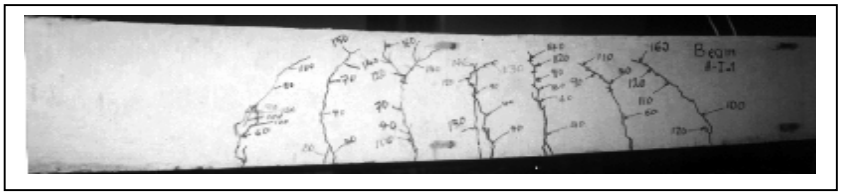

Side view for beam A-1-1

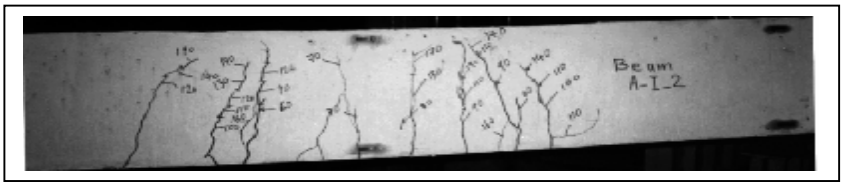

Side view for beam A-1-2

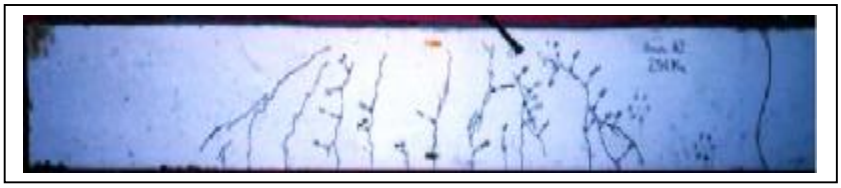

Side view for beamA-2

Side view for beamA-3

Figure (11) Crack patterns for beams in group A

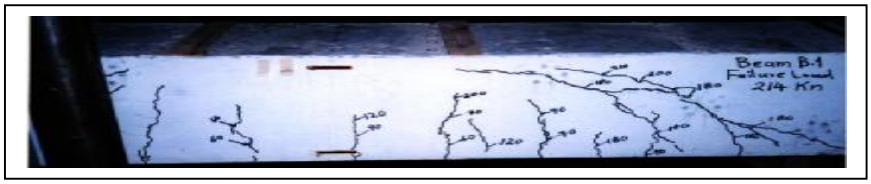

Side view for beam B-1

Side view for beamB-2

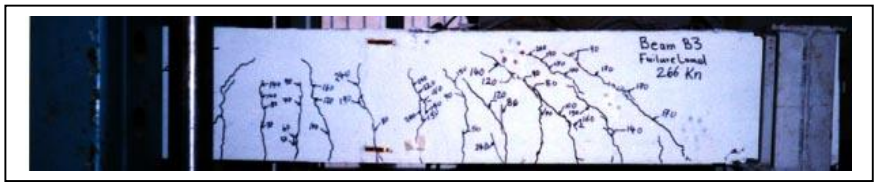

Side view for beam B-3

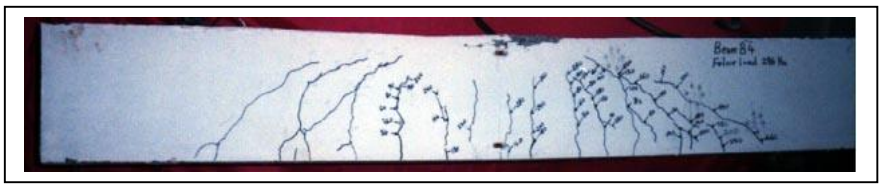

Side view for beam B-4

Figure (12) Crack patterns for beams in group B